JB
Journals.ASM.org

Signal Perception by the Secretion Stress-Responsive CssRS Two-Component System in *Bacillus subtilis*

David Noone, Eric Botella, Clodagh Butler, Annette Hansen,* Inga Jende, and Kevin M. Devine

Smurfit Institute of Genetics, Trinity College Dublin, Dublin, Ireland

The CssRS two-component system responds to heat and secretion stresses in *Bacillus subtilis* by controlling expression of HtrA and HtrB chaperone-type proteases and positively autoregulating its own expression. Here we report on the features of the CssS extracellular loop domain that are involved in signal perception and on CssS subcellular localization. Individual regions of the CssS extracellular loop domain contribute differently to signal perception and activation. The conserved hydrophilic 26-amino-acid segment juxtaposed to transmembrane helix 1 is involved in the switch between the deactivated and activated states, while the conserved 19-amino-acid hydrophobic segment juxtaposed to transmembrane 2 is required for signal perception and/or transduction. Perturbing the size of the extracellular loop domain increases CssS kinase activity and makes it unresponsive to secretion stress. CssS is localized primarily at the septum but is also found in a punctate pattern with lower intensity throughout the cell cylinder. Moreover, the CssRS-controlled HtrA and HtrB proteases are randomly distributed in foci throughout the cell surface, with more HtrB than HtrA foci in unstressed cells.

Two-component signal transduction systems are the predominant mechanism by which bacteria sense and respond to prevailing conditions. The prototypical system consists of two proteins, a sensor kinase and a response regulator, that are usually encoded by genes within the same operon (for reviews, see reference 19). In response to a specific signal(s), the sensor kinase autophosphorylates a histidine residue and activates its cognate response regulator by transfer of the phosphoryl group to a conserved aspartate residue. For the transcription factor class of response regulators (the majority), phosphorylation usually increases their binding affinity for specific DNA sequences, thereby directing a characteristic spectrum of transcriptional changes within the cell. Two-component systems (TCS) function as cognate pairs ensuring that the elicited cellular response is appropriate to the stimulus perceived (for reviews, see references 14 and 27).

Our understanding of signal perception by sensor kinases lags significantly behind understanding of other aspects of two-component-system function. While the stimulus to which an individual two-component system responds is often known (e.g., phosphate limitation or altered osmolarity), the signal perceived by the histidine kinase is usually unknown. Identifying these signals is a formidable challenge because of the multitude of stimuli that can be detected and the highly variable nature of sensing domains. While classification of histidine kinases based on the organization of their sensing domains has provided some insight into the cellular compartment from which a signal emanates, the nature of the signal and the mechanism of signal perception are known for only a very few TCS (27, 31). Perhaps the best characterized are the CitA and DcuS sensor kinases that detect citrate and other C4-dicarboxylates. Sensor kinase activation is achieved by direct ligand binding to PAS domain-like motifs in the periplasmically located sensing domains (15, 25, 41). The sensing domains of the BvgS and EvgS sensor kinases display similarity to those of high-affinity periplasmic solute binding proteins, suggesting a direct interaction with an as-yet-unidentified ligand (4, 8). Other sensor kinases with identified signals include FixL, whose activity is controlled by reversible oxygen binding to a heme cofactor bound to a PAS domain, ArcB, whose activity is controlled by reversible disulfide bond formation, and DesK, whose activity is controlled by membrane fluidity (for a review, see reference 27). The potential complexity of signal perception is indicated by the WalRK (YycFG, VicKR, and MicAB) two-component system that coordinates cell wall metabolism and cell division in *Bacillus subtilis* (5, 11, 20). In addition to a PAS domain in the extracellular loop, WalK has a second cytoplasmically located PAS domain that mediates WalK translocation to the septum to make specific interactions with the divisome and two auxiliary proteins, YycH and YycI, that modulate WalK activation through intramembrane interactions (12, 13, 46, 47, 49). Thus, the level of WalK kinase activity is a function of the integration of activating and inhibiting signals potentially emanating from three cellular compartments. However, the accepted view of extracytoplasmic domains functioning in signal perception is challenged by the finding that an *Escherichia coli envZ* null mutant can be complemented by a homologous EnvZ from *Xenorhabdus nematophilus* lacking a periplasmic-sensing domain (29).

The CssRS two-component system is one of the mechanisms by which *B. subtilis* detects and responds to cell envelope stress (9, 22, 23, 51). CssS is a typical sensing kinase with two transmembrane domains flanking an extracellular loop of 137 amino acids and is induced in response to high-level production of homologous or heterologous proteins and by heat stress (35, 36, 51). Translocation of secreted proteins is required for induction, although the intensity of the response is not directly proportional to the level of heterologous proteins produced (51). The CssRS regu-

Received 8 July 2011 **Accepted** 25 January 2012
Published ahead of print 3 February 2012
Address correspondence to David Noone, dnoone@tcd.ie.
* Present address: Novozymes, Bagsvaerd, Denmark.
D.N., E.B., and C.B. contributed equally to this article.

doi:10.1128/JB.05767-11

lon is small: transcriptome analysis shows it to contain only the *cssRS*, *htrA*, and *htrB* operons (23). A subsequent study suggested that *citM*, *ylxF*, *yloA*, and *ykoJ* expression is also regulated in a CssRS-dependent manner, although the putative CssR binding sequence is not evident in the promoters of these operons (30). The response to the activating signal is amplified by positive autoregulation, leading to increased CssRS expression and expression of the HtrA and HtrB chaperones-proteases that refold or degrade misfolded proteins within the cell envelope. Both proteases have single transmembrane domains and are probably located at the outer surface of the plasma membrane, although HtrA also accumulates in the culture medium in a truncated form (2). CssRS is also implicated in the mechanism by which peptidoglycan recognition proteins (PGLYRPs) kill bacterial cells and in the cellular response to rhamnolipoid biosurfactants (24, 50). The CssRS system of *B. subtilis* has many similarities to the Cpx system of *Escherichia coli*, to the extent that they might be considered functional homologues (39, 43). The Cpx system comprises a two-component system (CpxA kinase and CpxR response regulator) and CpxP, a small periplasmically located protein that negatively regulates CpxA activity (39, 43). The Cpx system is induced by envelope stress instigated by stimuli such as alkaline stress or misfolding of some pilin proteins (43). Genetic analysis shows the cognate stimulus to be sensed by the CpxA periplasmic loop domain: gain-of-function mutations cluster in locations adjacent to transmembrane helices 1 and 2 and to regions within the loop interior (38). Mechanistically, the evidence suggests that detection of the cognate stimulus alters the autokinase/phosphatase ratio of CpxA: under activating conditions, the kinase activity predominates, whereas the phosphatase activity predominates in the absence of a stimulus (38).

We chose to investigate signal perception by the CssRS two-component system of *B. subtilis*, reasoning that the nature of the signal would be amenable to genetic analysis similar to that performed on the Cpx system (38). Overexpression of heterologous proteins is an activating stimulus for CssS, suggesting that the signal detected by the extracellular loop domain may emanate from some aspect of the secretion apparatus or process or the accumulation of misfolded proteins. Therefore, we sought to identify the features of the CssS extracellular loop domain that are involved in signal perception and to establish the CssS cellular location. Our results show that two regions of the extracellular loop domain have distinct roles in signal perception: the region adjacent to transmembrane helix 1 functions in the switch between the deactivated and activated states, while the region adjacent to transmembrane helix 2 is required for signal perception and/or transduction. Moreover, the CssS kinase is localized at the septum and is distributed throughout the cell cylinder in a punctate manner.

MATERIALS AND METHODS

Bacterial growth conditions. Bacterial strains and plasmids used in this study are listed in Table 1. *E. coli* strain TG1 and *B. subtilis* strains were routinely maintained and propagated on Luria Bertani (LB) supplemented with agar (Becton Dickinson, Cockeysville, MD) (1.5% wt/vol) as appropriate and grown at 37°C (33). *E. coli* and *B. subtilis* transformations were performed as described previously (1, 44). Additions to growth media were at the following concentrations: X-Gal (5-bromo-4-chloro-3-indolyl-ß-D-galactopyranoside), 100 μg/ml; ampicillin, 100 μg/ml; chloramphenicol, 5 μg/ml; erythromycin, 1.0 μg/ml; spectinomycin, 100 μg/ml; kanamycin, 10 μg/ml; starch, 1%.

DNA manipulation and transformation. Standard procedures for DNA manipulation and analysis were used (44). *E. coli* strain TG1 (16) was used as the host for all plasmid constructions. Oligonucleotides used in this study are listed in Table 2 and were purchased from Eurofins MWG (Ebersberg, Germany). Restriction enzymes, DNA ligase, and DNA polymerases were purchased from New England BioLabs (Beverly, MA) and from Boehringer (Mannheim, Germany). Chromosomal and plasmid DNA was purified using columns purchased from Genomed Inc. (St. Louis, MO) and Qiagen Ltd. (Crawley, United Kingdom). Verification of strains and plasmid constructs was performed by sequencing, Southern analysis, and diagnostic PCR as appropriate.

Strain and plasmid construction. Strain CB1 (Δ*cssS*), which has the *cssS* gene precisely replaced with the spectinomycin resistance gene, was constructed by integration of plasmid pCB101 into the chromosome of strain 168 by a double-crossover event, selecting for spectinomycin resistance. Plasmid pCB101 was constructed by cloning a C-terminal fragment (283 bp, including the stop codon) of *cssR* (generated by PCR using oligonucleotides FRS1 and RRS2) and a fragment (296 bp) of the *yuxN* promoter (generated by PCR using oligonucleotides FRS3 and RRS4) into the EcoRI and HincII sites, respectively, of plasmid pDG1726 flanking the spectinomycin gene. Plasmid pCB90 was constructed as follows: a 788-bp fragment encoding the *cssS* transmitter domain (including the downstream terminator) was amplified using primers FRS5 and RRS6 and was cloned into the XbaI site of a pDG641 derivative (the HindIII site outside the multiple cloning site is inactivated) 5′ to the *erm* gene. A second fragment (296 bp, encompassing the *yuxN* promoter region described above) was generated using primers FRS3 and RRS4 and cloned into the NdeI site of the pDG641 derivative 3′ to the *erm* gene. The resulting plasmid, pCB90, was used to introduce all mutations into the *cssS* gene. Plasmid pCBrs2 (encoding a *cssS* gene with transmembrane helix 1 deleted) was constructed by generating two PCR fragments by PCR using primer pair FRS1 and RRS9 and primer pair FRS10 and RRS11B. The first fragment encodes the *cssR* C terminus and the region up to the first *cssS* transmembrane domain. The second fragment encodes the region from the end of the first transmembrane domain to the beginning of the *cssS* transmitter domain. These two fragments were annealed, and a single fragment was generated by overlapping PCR using primer pair FRS1 and RRS11. The resulting fragment was digested with AgeI and HindIII and cloned into similarly digested pCB90, generating plasmid pCBrs2. Strain CB2 was generated by transformation with linearized pCBrs2 selecting for erythromycin resistance and spectinomycin sensitivity. A similar strategy was adopted to generate plasmid pCBrs3 (truncated extracellular loop) by the use of primer pair FRS1 and RRS13 and primer pair FRS12 and RRS11B. Plasmid pCBrs4 (deletion of sensing domain) was constructed using primer pair FRS1 and RRS14 and primer pair FRS15 and RRS6. The first fragment spanned the *cssR* C terminus up to the beginning of the first *cssS* transmembrane domain, while the second fragment extended from the end of the second transmembrane domain up to the end of the *cssS* gene, including the stop codon and terminator. The two fragments were combined by overlapping PCR and cloned into the XbaI site of pCB90H3. The promoter region of the downstream *yuxN* gene (amplified by FRS3 and RRS4) was then cloned into the same vector using NdeI. Plasmid pCBrsWT was similarly constructed using primer pair FRS1 and RRS6 to generate the *cssR cssS* fragment and primer pair FRS3 and RRS4 to generate the *yuxN* promoter fragment. Strains CB3, CB4, and CB5 were generated by transforming strain CB1 with linearized plasmids pCBrs3, pCBrs4, and pCBrsWT, respectively, and integration by double-crossover events into the chromosome. A P_{htrA}-*lacZ* transcriptional fusion encoded on plasmid pCH9 was introduced into strains CB1, CB2, CB3, CB4, CB5, and 168 (linearized pCH9; integration by double-crossover events into the *amyE* locus), generating strains CB6, CB8, CB9, CB10, CB11, and CB7, respectively. Plasmid pKTH10 (encoding *amyQ* from *B. amyloliquefaciens*) was transformed into strains CB7, CB11, and CB9 to generate strains CB12, CB13, and CB14, respectively.

The extracellular loop region of CssS was randomly mutated using the

TABLE 1 Strains and plasmids used in this study

Strain or plasmid	Relevant properties	Reference
E. coli strain		
TG-1	*supE thi-1* Δ(*lac-proAB*) Δ(*mcrB-hsdSM*) [F′ *traD36 proAB lacI*^{q}*Z*ΔM15]	44
B. subtilis strains		
168	*trpC2*	28
CB1	Δ*cssS spc* replacement of *cssS* with spectinomycin resistance gene	This work
CB2	*cssS1 erm* CssS with transmembrane 1 (TM1) deleted	This work
CB3	*cssS2 erm* CssS^{TEL} with truncated extracellular loop	This work
CB4	*cssS3 erm* CssS with entire sensing domain deleted	This work
CB5	*cssS4 erm* wild-type CssS regenerated using pCBrsWT	This work
CB6	CB1 *amyE*::pCH9 containing P$_{htrA}$-*lacZ* transcriptional fusion at *amyE* locus	This work
CB7	*amyE*::pCH9 wild-type 168 with P$_{htrA}$-*lacZ* transcriptional fusion at *amyE* locus	This work
CB8	CB2 *amyE*::pCH9 containing P$_{htrA}$-*lacZ* transcriptional fusion at *amyE* locus	This work
CB9	CB3 *amyE*::pCH9 containing P$_{htrA}$-*lacZ* transcriptional fusion at *amyE* locus	This work
CB10	CB4 *amyE*::pCH9 containing P$_{htrA}$-*lacZ* transcriptional fusion at *amyE* locus	This work
CB11	CB5 *amyE*::pCH9 containing P$_{htrA}$-*lacZ* transcriptional fusion at *amyE* locus	This work
CB12	CB7 transformed with pKTH10 overexpressing AmyQ	This work
CB13	CB11 transformed with pKTH10 overexpressing AmyQ	This work
CB14	CB9 transformed with pKTH10 overexpressing AmyQ	This work
HA58	*cssS5 erm* CssS with amino acids 40–60 deleted from extracellular loop region	This work
HA64	*cssS6 erm* CssS with amino acids 85–105 deleted from extracellular loop region	This work
HA60	*cssS7 erm* CssS with amino acids 130–150 deleted from extracellular loop region	This work
HA70	HA58 containing pKTH10 overexpressing AmyQ	This work
HA73	HA64 containing pKTH10 overexpressing AmyQ	This work
HA71	HA60 containing pKTH10 overexpressing AmyQ	This work
HA54	*cssS8 erm* CssS with L33Q substitution	This work
HA62	*cssS9 erm* CssS with N47Y substitution	This work
HA56	*cssS10 erm* CssS with Q49H substitution	This work
HA68	HA54 containing pKTH10 overexpressing AmyQ	This work
HA72	HA62 containing pKTH10 overexpressing AmyQ	This work
HA69	HA56 containing pKTH10 overexpressing AmyQ	This work
EB66	Wild-type strain 168 carrying a CssS-3×-C-Myc tag at the *cssS* locus	This work
DN1980	CssS D153A *amyE*::P$_{htrA}$-*lacZ*	This work
DN1980Q	CssS D153A + pKTH10 *amyE*::P$_{htrA}$-*lacZ*	This work
DN1981	CssS S154A *amyE*::P$_{htrA}$-*lacZ*	This work
DN1981Q	CssS S154A + pKTH10 *amyE*::P$_{htrA}$-*lacZ*	This work
DN1982	CssS Y155A *amyE*::P$_{htrA}$-*lacZ*	This work
DN1982Q	CssS Y155A + pKTH10 *amyE*::P$_{htrA}$-*lacZ*	This work
DN1983	CssS R156A *amyE*::P$_{htrA}$-*lacZ*	This work
DN1983Q	CssS R156A + pKTH10 *amyE*::P$_{htrA}$-*lacZZ*	This work
DN1984	CssS D157A *amyE*::P$_{htrA}$-*lacZ*	This work
DN1984Q	CssS D157A + pKTH10 *amyE*::P$_{htrA}$-*lacZ*	This work
DN1985	CssS D158A *amyE*::P$_{htrA}$-*lacZ*	This work
DN1985Q	CssS D158A + pKTH10 *amyE*::P$_{htrA}$-*lacZ*	This work
DN1986	CssS with amino acids Δ153–159 deleted *amyE*::P$_{htrA}$-*lacZ*	This work
DN1986Q	CssS with amino acids Δ153–159 deleted + pKTH10 *amyE*::P$_{htrA}$-*lacZ*	This work
DN1987	CssS L33Q R156A *amyE*::P$_{htrA}$-*lacZ*P$_{htrA}$-*lacZ*	This work
DN1987Q	CssS L33Q R156A + pKTH10 *amyE*::P$_{htrA}$-*lacZ*	This work
DN1988	CssS with amino acids 59-80 replaced by a 3× FLAG *amyE*::P$_{htrA}$-*lacZ*	This work
DN1988Q	CssS with amino acids 59-80 replaced by a 3× FLAG + pKTH10 *amyE*::P$_{htrA}$-*lacZ*	This work
DN1990	CssS with amino acids 62-80 replaced by a 3× FLAG *amyE*::P$_{htrA}$-*lacZ*	This work
DN1990Q	CssS Δ62-80::3× FLAG +pKTH10 *amyE*::P$_{htrA}$-*lacZ*	This work
168D	168 *cssS*-spec *amyE*::P$_{htrA}$-*lacZ*	This work
168DQ	168 *cssS*-spec *amyE*::P$_{htrA}$-*lacZ* pKTH10	This work
168E	168 Pspac-*cssRS amyE*::P$_{htrA}$-*lacZ*	This work
168EQ	168 Pspac-*cssRS amyE*::P$_{htrA}$-*lacZ* pKTH10	This work
HA54C	HA54 Pspac-*cssRS* ΔErm::spec	This work
HA54CQ	HA54C Pspac-*cssRS* pKTH10	This work
HA62C	HA62 Pspac-*cssRS* ΔErm::spec	This work
HA62CQ	HA62C Pspac-*cssRS* pKTH10	This work

(Continued on following page)

TABLE 1 (Continued)

Strain or plasmid	Relevant properties	Reference
DN1980C	DN1980 Pspac-*cssRS* ΔErm::spec	This work
DN1980CQ	DN1980C Pspac-*cssRS* pKTH10	This work
DN1984C	DN1984 Pspac-*cssRS* ΔErm::spec	This work
DN1987C	DN1987 Pspac-*cssRS* ΔErm::spec	This work
DN1987CQ	DN1987C Pspac-*cssRS* pKTH10	This work
CB9H	CB9 CssSH250A	This work
CB9HQ	CB9H pKTH10	This work
Plasmids		
pDG641	pJRD184 derivative encoding ampicillin and erythromycin resistance	18
pCB90H3	pDG641 with the HindIII site outside the MCS inactivated	This work
pDG1726	pSB119 derivative	18
pKTH10	Contains *amyQ* gene from *B. amyloliquefaciens*	37
pM4xZ	pMUTin4 derivative lacking *lacZ* gene	B. Jester, unpublished data
pCB101	pDG1726 derivative with *cssR* and *yuxN* fragments flanking *spc* gene	This work
pCB90	pDG641 derivative with DNA fragments encoding the *cssS* transmitter domain and the *yuxN* promoter regions flanking the *erm* gene	This work
pCBrs2	pCB90 derivative with *cssS1* gene (CssS with Tm1 deleted)	This work
pCBrs3	pCB90 derivative with *cssS2* gene ($CssS^{TEL}$ with truncated loop)	This work
pCBrs4	pCB90 derivative with *cssS3* gene (CssS with sensing domain deleted)	This work
pCBrsWT	pCB90 derivative with wild-type *cssS* gene (wild-type CssS)	This work
pCH9	contains P_{htrA}-*lacZ* fusion	C. Hough, unpublished data
pHA54	pCB90 derivative with *cssS8* encoding CssS with L33Q substitution	This work
pHA62	pCB90 derivative with *cssS* encoding CssS with N47Y substitution	This work
pHA56	pCB90 derivative with *cssS10* encoding CssS with Q49H substitution	This work
pHA58	pCB90 derivative with *cssS5* encoding CssS with amino acids 40–60 deleted	This work
pHA60	pCB90 derivative with *cssS7* encoding CssS with amino acids 130–150 deleted	This work
pHA64	pCB90 derivative with *cssS6* encoding CssS with amino acids 85–105 deleted	This work
pDN1980	pCB90 derivative with *cssS* encoding CssS with D153A substitution	This work
pDN1981	pCB90 derivative with *cssS* encoding CssS with S154A substitution	This work
pDN1982	pCB90 derivative with *cssS* encoding CssS with Y155A substitution	This work
pDN1983	pCB90 derivative with *cssS* encoding CssS with R156A substitution	This work
pDN1984	pCB90 derivative with *cssS* encoding CssS with D157A substitution	This work
pDN1985	pCB90 derivative with *cssS* encoding CssS with D158A substitution	This work
pDN1986	pCB90 derivative with *cssS* encoding CssS with amino acids 153–159 deleted	This work
pDN1987	pCB90 derivative with *cssS* encoding CssS with L33Q and R156A substitutions	This work
pDN1988	pCB90 derivative with CssS amino acids 59–80 replaced by 3× FLAG motif	This work
pDN1990	pCB90 derivative with CssS amino acids 62–80 replaced by 3× FLAG motif	This work
pDNH250A	pCBrs3 containing the mutation CssSH250A	This work
pDN3020	pM4xZ with 5′ 300 bp of *cssR*, including ribosome binding site	This work
pEB34	pMyc2 derivative with *cssS* cloned to produce a CssS-3× c-Myc-tagged protein	This work

error-prone DNA polymerase Mutazyme II (Stratagene, United Kingdom) as follows: a DNA fragment extending from the *cssR* gene to the end of the first CssS transmembrane helix domain was generated by PCR using oligonucleotides FRS1 and RVmut and Phusion high-fidelity polymerase (Finnzyme, Vantaa, Finland). A second fragment was amplified from the first transmembrane domain to the beginning of the region of *cssS* that is contained in pCB90 by the use of FWmut and RRS11B and the Mutazyme II error-prone polymerase (pooled and used in 6 separate reactions). These two fragments were joined by overlapping PCR, eluted using a gel, cloned into the AgeI and HindIII sites of pCB90, and transformed into *E. coli* Tg1. Plasmid was prepared from pooled *E. coli* transformants, linearized by the use of ClaI, and transformed into CB6 (Δ*cssS amyE*::P_{htrA}-*lacZ*) as previously described. Colonies were screened for β-galactosidase activity on X-Gal-containing agar plates. The loop regions of *cssS* genes encoded in the blue transformants were sequenced (MWG-Biotech AG, Ebersberg, Germany). This strategy identified amino acids important for CssS function. To ensure that the amino acid changes were the only ones present in the CssS protein, strains with these amino acid changes were reconstructed using site-directed mutagenesis. Strains HA54 (CssS L33Q), HA62 (CssS N47Y), and HA56 (CssS Q49H) were constructed as previously described using pCB90, and two DNA fragments were generated from each strain by the use of primer pair FRS1 and cssSR6 and primer pair cssSF5 and RVmut (HA54), primer pair FRS1 and cssSR4 and primer pair cssSF3 and RVmut (HA62), and primer pair FRS1 and cssSR8 and primer pair cssSF7 and RVmut (HA54). Each pair of fragments was joined by overlapping PCR using the outside primers (FRS1 and RVmut) and cloned into pCB90. Integration of the resultant pHA54, pHA62, and pHA56 plasmids into the chromosome of *B. subtilis* 168 yielded strains HA54, HA62, and HA56, respectively. Plasmid pKTH10 was then transformed into strains HA54, HA62, and HA56 to generate strains HA68, HA72, and HA69, respectively. The pCB90-based strategy outlined above was also used to generate deletions in subregions of the CssS extracellular loop as follows: to make a deletion of amino acids 40 to 60, two DNA fragments were generated using primer pair FRS1 and cssSR10 and primer

TABLE 2 Oligonucleotides used in this study

Name	Sequence (5′–3′)
FRS1	CGGAATTCTAGACCGGTCGCGAGGTCTATGACGAAAAC
RRS2	CGGAATTCTAGACCGGTTCATGATGACATCATCCTG
FRS3	CGGGATCCATATGTTTGAGCGGCTGTTTGCATTG
RRS4	CGGGATCCATATGGAGGCCTGCTAGGATATG
FRS5	GCTCTAGACCGGTCGAGACGTTGATCGGCAAGCTTGGCCATAC
RRS6	GCTCTAGACAGAGATTTTAACGGCTATTC
RRS7	CGTTTTTAAATCAGCAGAGATAT
FRS8	ATATCTCTGCTGATTTAAAAACG
RRS9	CGTGTTTGAAAATAACACCTGAAACGCGAGCGGCTT
FRS10	GTGTTATTTTCAAACACG
RRS11B	GCACAAGCTTTTGGCGCA
FRS12	GACGATTTGGCCTATACC
RRS13	GGTATAGGCCAAATCGTCATTAGTGAAAAAATCTCG
RRS14	AGGCCTTGATAAATACTTGTTTTTCATGATGACATC
FRS15	AAGTATTTATCAAGGCCT
RVmut	ATCTCGCAGCGTGTTTGA
cssSF3	CGATTGAATATGAGCAGCATG
cssSF5	CACGCAGCGAGATTTTTTC
cssSF7	GAAAATGAGCACCATGTTCTG
cssSR4	CATGCTGCTCATATTCAATCG
cssSR6	GAAAAAATCTCGCTGCGTG
cssSR8	CAGAACATGGTGCTCATTTTC
cssSF9	CTGCGAGATTTTTTCACTAATATTGAAAGGCGCTATTACAG
cssSR10	ATTAGTGAAAAAATCTCGCAG
cssSF11	GTACAGCACGTGCTCCTTAAGGTGTACAAGCTGGCTG
cssSR12	AAGGAGCACGTGCTGTAC
cssSF13	CGACGTCAATGGAGAGAAAGCGCTTGATTCTTATCGGG
cssSR14	TTTCTCTCCATTGACGTCG
RVmut	ATCTCGCAGCGTGTTTGA
FWmut	TCAAACACGCTGCGAGAT
CssR5′pET	GGAATTCCATATGTTGTCATACACCATTTATCTAG
CssR3′pET	CCGCTCGAGTGATGACATCATCCTGTAGCC
CssS5′pET	GGAATTCCATATGAGGCCTCTTGTATCATTTG
Css3′SpET	CCGCTCGAGTTTTGGCACTGCTATGCGG
OE148	CCCAAGCTTCGACATGTTCAGTATTGTGGA
OE149	CGGGATCCTTTTGGCACTGCTATGCGGTA
OE151	CTCGCACCGCTCTAGAAAGC
OE152	AAAACTGCAGGCTCGTCCTGAATGATATGC
cssSD153AFwd	CGCGCTTGCTTCTTATCGGGACGATTTG
cssSD153ARev	CAAATCGTCCCGATAAGAAGCAAGCGC
cssSS154AFwd	CGCGCTTGATGCTTATCGGGACGATTTG
cssSS154ARev	CAAATCGTCCCGATAAGCATCAAGCGCG
cssSY155AFwd	CGCGCTTGATTCTGCTCGGGACGATTTG
cssSY155ARev	CAAATCGTCCCGAGCAGAATCAAGCGCG
cssSR156AFwd	CTTATGCGGACGATTTGGCCTATACC
cssSR156ARev	GGTATAGGCCAAATCGTCCGCATAAG
cssSD157AFwd	CTTATCGGGCCGATTTGGCCTATACC
cssSD157ARev	GGTATAGGCCAAATCGGCCCGATAAG
cssSD158AFwd	CTTATCGGGACGCTTTGGCCTATACC
cssSD158ARev	GGTATAGGCCAAAGCGTCCCGATAAG
cssSΔ7Fwd	GCCTATACCTTGTTCAAACAGC
cssSΔ7Rev	CAAGGTATAGGCAAGCGCGTAAGAGAGC
cssSHA54combinF	GGTGTACAAGCTGGCTGATAA
cssSHA54combinR	TTATCAGCCAGCTTGTACACC
cssSΔ22F	GACTACAAAGACCATGACGGTGATTATAAAG
cssSΔ22R	CGTCATGGTCTTTGTAGTCTGGCAGGCGGTACTCTGTCAG
cssSFLAGFwd	GATTATAAAGATCATGACATCGACTACAAGGATGACGATGACAAGCACGTGCTCCTTCCTGAAAAT
cssSFLAGRev	CATGATCTTTATAATCACCGTCATGGTCTTTGTAGTCAATCGAACCTGGCAGGCGGTAC
cssSdelERmUPfc	CTTGTATCATTTGAAAAACACGTC
SpecdelErmUPR	CGTTACGTTATTAGCGAGCCAGTCATATCCGAAGCAGACCTTGTCAGAG
SpecdelEmDWNF	CAATAAACCCTTGCCCTCGCTACGGAAAGGGTGGAACCATTGAAGG
cssSdelErmDWNRc	AAAGGCGTAATAGGAAGAACGGC
spec-fwd	GACTGGCTCGCTAATAACGTAACGTGACTGGCAAGAG
spec-rev	CGTAGCGAGGGCAAGGGTTTATTGTTTTCTAAAATCTG
cssRSpM4F	GCCCAAGCTTTGACGTTGAAAGGATGTGAAGAGC
cssRSpM4R	CGGGATCCTGTAGTCATTGCTGCCAAGCTCTAAGC
cssSH250AF	GCTGATTTAAAAACGCCGGTCATGGTC
cssSH250AR	AGAGATATTTTGCAATAGAGTTCTTTCTG

pair cssSF9 and RVmut; to delete amino acids 85 to 105, two DNA fragments were generated using primer pair FRS1 and CssSR12 and primer pair cssSF11 and cssSR12; and to delete amino acids 130 to 150, two DNA fragments were generated using primer pair FRS1 and cssSR14 and primer pair cssSF13 and RVmut. Each pair of DNA fragments was joined by overlapping PCR, digested with AgeI and HindIII, and cloned into similarly digested pCB90 plasmids. This generated plasmids pHA58 (deletion of amino acids 40 to 60), pHA64 (deletion of amino acids 85 to 105), and pHA60 (deletion of amino acids 130 to 150). These plasmids were transformed into CB6 to generate strains HA58, HA64, and HA60, respectively. Strains HA58, HA64, and HA60 were then transformed with plasmid pKTH10 to generate strains HA70, HA73, and HA71, respectively.

Strains DN1980 through DN1986 and strain DN1990 were constructed using pCB90 as previously described. Each *cssS* allele was generated by overlapping PCR using two DNA fragments each that were generated by the following primer pairs: for strain DN1980, primer pair FRS1 and cssS_D153ARev and primer pair cssS_D153AFwd and RRS11b; for strain DN1981, primer pair FRS1 and cssS_S154ARev and primer pair cssS_S154AFwd and RRS11b; for strain DN1982, primer pair FRS1 and cssS_Y155ARev and primer pair cssS_Y155AFwd and RRS11b; for strain DN1983, primer pair FRS1 and cssS_R156ARev and primer pair cssS_R156AFwd and RRS11b; for strain DN1984, primer pair FRS1 and cssS_D157ARev and primer pair cssS_D157AFwd and RRS11b; for strain DN1985, primer pair FRS1 and cssS_D158ARev and primer pair cssS_D158AFwd and RRS11b; for strain DN1986, primer pair FRS1 and cssSΔ7Rev and primer pair cssSΔ7Fwd and RRS11b; and for DN1990, primer pair FRS1 and cssS3xFLAGRev and primer pair cssS3xFLAGFwd and RRS11B. Each fragment pair was joined using the outside primers (FRS1 and RRS11B) and cloned into pCB90. Integration of the resultant pDN1980, pDN1981, pDN1982, pDN1983, pDN1984, pDN1985, pDN1986, and pDN1990 plasmids into the chromosome of *B. subtilis* strain CB6 yielded strains DN1980, DN1981, DN1982, DN1983, DN1984, DN1985, DN1986, and DN1990, respectively. To generate a secretion stress, plasmid pKTH10 was transformed into each of these strains to generate strains DN1980Q, DN1981Q, DN1982Q, DN1983Q, DN1984Q, DN1985Q, DN1986Q, and DN1990Q. Plasmid pDN1987 was constructed as described above using primer pair FRS1 and cssSHA54combinRev and primer pair cssSHA54combinF and RRS11b and plasmids pHA54 and pDN1983 as templates for the respective upstream and downstream fragments. Plasmid pDN1988 was constructed as described above using primer pair FRS1 and cssSΔ22R and primer pair cssSΔ22F and RRS11b and plasmid pDN1990 as the template. Integration of the resultant pDN1987 and pDN1988 plasmids into the chromosome of *B. subtilis* CB6 yielded strains DN1987 and DN1988. Plasmid pKTH10 was then transformed into strains DN1987 and DN1988 to generate strains DN1987Q and DN1988Q.

Strain EB66 containing c-Myc-tagged CssS was constructed by transforming wild-type strain 168 with plasmid pEB34. Plasmid pEB34 was constructed by amplifying a DNA fragment encoding the 3′ end of *cssS* with primers OE148 and OE149 and cloning the fragment into the HindIII-BamHI sites of plasmid pMyc2 (laboratory stock), which encodes a polylinker followed by a 3× c-Myc tag. The translational *cssS*-3×-C-Myc fusion generated in pMyc2 was then amplified using primers OE151 and OE152 and cloned into the XbaI-PstI sites of pDG780 (17, 18) to obtain pEB34. All plasmids were verified by sequencing.

To express *cssS* alleles under the control of the IPTG (isopropyl-β-D-thiogalactopyranoside)-inducible P_{spac} promoter (thereby eliminating the positive-feedback loop), strains were constructed in which the erythromycin resistance gene (*erm*) downstream of the *cssS* terminator was replaced by a spectinomycin resistance gene (*spc*). This was achieved by long flanking homology PCR (LFH-PCR) using upstream (UP) and downstream (DWN) fragments of ~800 bp of homologous DNA flanking the *erm* resistance gene as previously described (32). The 5′ end of the upstream fragment did not extend to the mutated region of the *cssS* gene in these strains. Upstream and downstream homologous DNA fragments were amplified using primer pair cssSdelERmUPfc and SpecdelErmUPR and primer pair SpecdelEmDWNF and cssSdelErmDWNRc, respectively. These fragments were joined to a DNA fragment carrying the *spc* resistance gene previously amplified using primers spec-fwd and spec-rev from pDG1726. Successful exchange of antibiotic cassettes was confirmed by loss of erythromycin resistance and gain of spectinomycin resistance in transformed strains. Expression of the *cssRS* operon in the relevant strains was then placed under the control of the IPTG-inducible P_{spac} promoter by transforming each strain with plasmid pDN3020, with insertion occurring by a Campbell-type event. Plasmid pDN3020 was constructed by cloning a 320-bp fragment, amplified using primers cssRSpM4F and cssRSpM4R, into HindIII-BamHI-digested plasmid pM4xZ, a version of pMUTIN4 that has the *lacZ* gene deleted. The *cssS* gene on the chromosome of all strains was sequenced to confirm that it contained the desired mutation(s).

The active-site histidine residue of CssS in strain CB9 was changed to alanine (strain CB9H H250A) by the use of site-directed mutagenesis of plasmid pCBrs3 and the 5′ phosphorylated primer pair cssSH250AF and cssSH250AR following the Phusion site-directed mutagenesis protocol (Fermentas GMBH, Germany). The mutated pDNH250A plasmid was sequenced to confirm that only the desired mutation was obtained. Transformation of strain CB6 with linearized plasmid pDNH250A generated strain CB9H (CssSH250A).

Secretion stress was induced by transforming plasmid pKTH10 into all relevant strains selecting for kanamycin resistance. Increased α-amylase production was confirmed by plating transformants on LB agar plates containing starch.

Antibody production, protein expression, and purification. DNA fragments encoding CssR and the intracellular domains of CssS were generated by PCR using primer pair CssR5′pET and CssR3′pET and primer pair CssS5′pET and CssS3′pET, respectively, digested with NdeI and XhoI, and cloned into similarly digested pET21b (Novagen), and the resultant plasmids were established in expression strain BL21(DE3). Expression of the proteins was induced by addition of 1 mM IPTG when a growing culture reached an optical density at 600 nm (OD_{600}) of 0.6 to 0.8. Cells were harvested by centrifugation at 3 h postinduction, resuspended in ice-cold lysis buffer (500 mM NaH_2PO_4, 300 mM NaCl, 20 mM imidazole, 0.1% [vol/vol] Tween), and lysed by treatment with lysozyme (1 mg/ml)–1% [vol/vol] protease inhibitor and sonicated. Cell debris was removed by centrifugation at 12,000 rpm for 30 min at 4°C. The supernatant was subjected to affinity chromatography on nickel^{2+}-nitrilotriacetic acid (Ni^{2+}-NTA) His·Bind resins (Novagen). Each protein was bound for 2 h and washed four times in buffer (50 mM NaH_2PO_4, 300 mM NaCl, 40 mM imidazole) containing 0.1% (vol/vol) Tween and four times without Tween. Proteins were eluted in buffer (50 mM NaH_2PO_4, 300 mM NaCl, 250 mM imidazole) containing 1% (vol/vol) protease inhibitor. Eluates were dialyzed overnight (20 mM Tris-HCl [pH 8.0], 300 mM NaCl, 50% [vol/vol] glycerol) and stored at −20°C. The purified CssR and ′CssS proteins were emulsified in Freund's complete adjuvant and injected into New Zealand White rabbits. Antibodies were immunoaffinity purified from the sera by the use of purified protein coupled to CNBr-activated Sepharose 4 FastFlow (Pharmacia) following the recommendations of the manufacturer. Antibodies were eluted using 0.2 M glycine (pH 2.2) into tubes containing 2 M Tris (pH 8.8) and desalted, and the buffer was exchanged using MicroSep concentration columns (Pall) into 1× phosphate-buffered saline (PBS) containing 40% glycerol, bovine serum albumin (BSA; 1 mg/ml), and 0.1% sodium azide, aliquoted, and stored at −20°C.

Western analysis. Western analysis was carried out as described previously (21).

Enzymatic assays. The specific activity of β-galactosidase was determined as previously described: 1 unit of activity is defined as the nanomoles of *o*-nitrophenyl-β-D-galactopyranoside (ONPG) hydrolyzed per minute per milligram of protein (35).

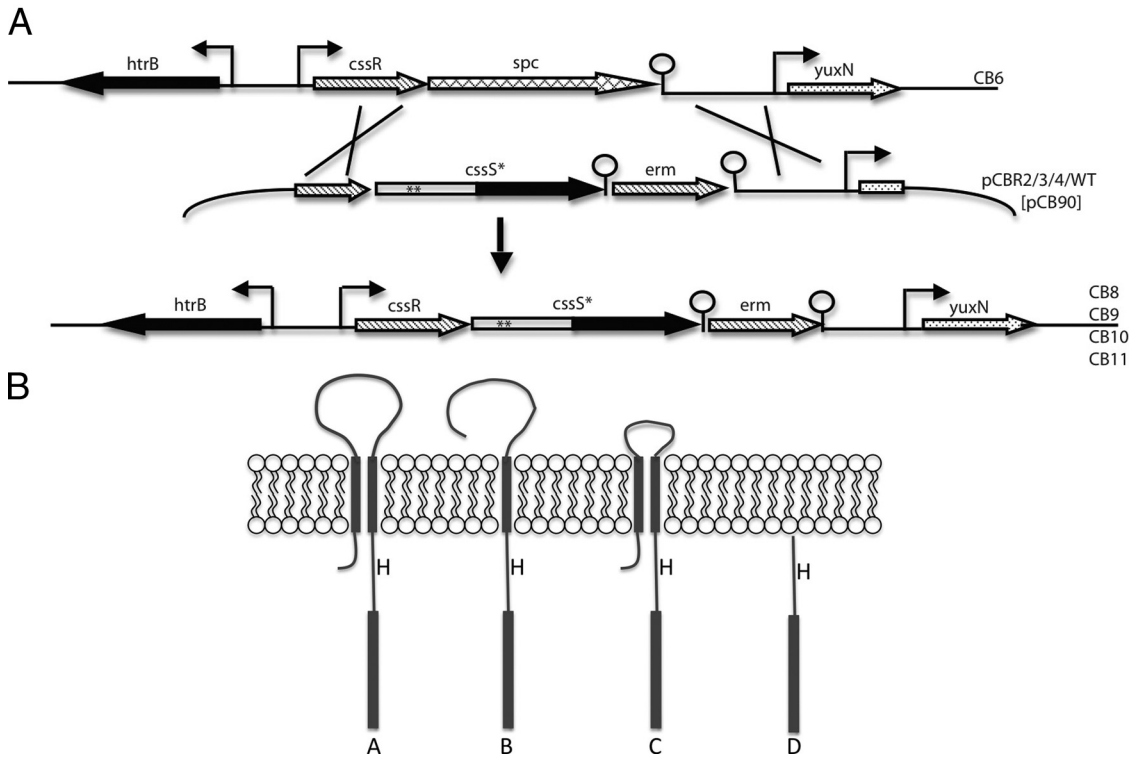

FIG 1 Schematic representation of the *in vivo* system developed to mutate the CssS extracellular loop domain without otherwise affecting the *cssRS* operon. (A) In strain CB6, the *cssS* gene is precisely replaced with the spectimomycin resistance gene (*spc*). Derivatives of plasmid pCB90 (pCBR2/3/4/WT), encoding mutated *cssS* genes (indicated by asterisks within the *cssS* arrow), were linearized and transformed into strain CB6. Integration into the chromosome occurs by a double-crossover event (indicated by pairs of large crosses) through homologous recombination between the chromosomal and plasmid-encoded *cssR* and *yuxN* promoter regions. The *cssRS* operon in the resulting strains (CB8, -9, -10, and -11) is precisely reconstituted and contains the designed *cssS* mutation in an otherwise unaltered operon. Horizontal arrows (individually filled) represent the genes at the *cssRS* locus. Bent arrows represent promoters, while lollipops represent terminators. Straight lines at the extremities represent chromosomes, whereas bent lines represent plasmids. (B) Schematic representation of the postulated structures of CssS with various regions deleted. The proteins are shown embedded in the lipid bilayer. Thick lines spanning the membrane represent transmembrane helices. Thick lines in the cytoplasm represent the HATPase domain, while H represents the active histidine site.

Immunofluorescence microscopy. Immunofluorescence microscopy was performed essentially as described previously (48). In brief, *B. subtilis* strains 168, HA54, and EB66 were grown in LB to an OD_{600} of 0.6 and fixed in 2.6% paraformaldehyde for 20 min at room temperature followed by 30 min on ice. Bacteria were washed three times in PBS buffer and resuspended at an OD_{600} of 0.4. Aliquots (20 μl) of the cell suspension were individually applied to a multiwell microscope slide that was pretreated with 0.1% (wt/vol) poly-L-lysine. The excess suspension was removed after 30 min, each well was washed three times with 20 μl of PBS, and 20 μl of GTE buffer (50 mM glucose, 20 mM Tris-HCl [pH 7.5], 10 mM EDTA) was then added to each well for 10 min. The adherent bacteria were then incubated with lysozyme (2 mg/ml) dissolved in GTE buffer for 2 min and washed 10 times with 20 μl of PBS buffer. Slides were immersed in ice-cold methanol for 5 min and allowed to dry completely. Samples were then rehydrated with 20 μl of PBS for 5 min and blocked with a solution of PBS supplemented with 2% BSA (PBS-BSA) for 20 min at room temperature. Wells were individually incubated with a 1:1,000 dilution (in PBS containing 2% BSA) of polyclonal HtrA and HtrB antibodies and with an 1:500 anti-c-myc monoclonal antibody (Invitrogen) for 1 h. Wells were then washed 10 times with 20 μl of PBS-BSA and incubated with anti-rabbit IgG conjugated to fluorescein (Sigma) at a 1:400 dilution in PBS-BSA for 1 h in the dark and washed again as previously described. An antifade solution containing 4′,6′diamidino-2-phenylindole (DAPI) (SlowFade Gold antifade; Invitrogen) was then applied. Samples were observed using an Olympus BX61 microscope, and images were collected and treated using Cell^P software version 3.3 (Olympus).

RESULTS

Development of a system to investigate the CssS extracellular loop domain *in vivo*. To accurately assess the physiological effect of mutating the CssS extracellular loop, we developed a system for routine mutation of this domain *in vivo* without otherwise perturbing the location or organization of the *cssRS* operon (Fig. 1A). In strain CB6, the *cssS* gene has been precisely replaced with the spectinomycin resistance gene (*spc*) and there is a P_{htrA}*lacZ* transcriptional fusion positioned at the *amyE* locus (not shown in Fig. 1A). Plasmid pCB90 contains the *cssS* transmitter domain (black arrow) and the *cssRS* operon terminator, downstream of which the erythromycin resistance (*erm*) gene and a region of the *yuxN* promoter are located (Fig. 1A). Several DNA fragments, each encoding the 3′ end of *cssR* (wild type) and a mutated *cssS*-sensing domain (box with asterisks), were generated by overlapping PCR and cloned into pCB90, thereby reconstituting a mutated *cssS* gene on the plasmids (pCBR2, -3, and -4 in Fig. 1A). The wild-type *cssS* gene was similarly reconstructed on plasmid pCB90 (pCBrsWT)—this is referred to as reconstituted wild-type CssS in this report to distinguish it from CssS in wild-type strain 168. Integration of each plasmid into the CB6 chromosome by a double-crossover event (selecting for erythromycin resistance and screening for spectinomycin sensitivity) transfers these (mutated)

TABLE 3 Activity of CssS sensor kinases measured by expression of the P_{htrA}-*lacZ* fusion

Strain	CssS protein[a]	Fold increase in β-galactosidase accumulation[b]
CB11	Reconstituted wild type	1
CB13	Reconstituted wild type + pKTH10	28
CB6	*cssS* gene deleted	1
CB8	CssS TM1 domain deleted (construct B)	2
CB10	Sensing domain deleted (construct D)	2
CB9	Loop domain of 20-aa length (construct C)	325
CB14	Loop domain of 20-aa length (construct C) + pKTH10	321
CB9H	Loop domain of 20 aa with H250A mutation	1
CB9HQ	Loop domain of 20 aa with H250A mutation + pKTH10	1

[a] Constructs B to D are shown in Fig. 1B. aa, amino acid.
[b] Normalized to the β-galactosidase accumulation in strain CB11 containing a reconstituted CssS protein generated using the system described for Fig. 1.

cssS genes into the chromosome and restores the normal *cssRS* operon configuration. The only change to the *cssRS* operon in these strains is the desired mutation in the region encoding the *cssS* extracellular loop domain (note that the *erm* gene is located downstream of the *cssRS* operon terminator). The effect of each mutation on CssS function was determined by monitoring expression of the P_{htrA}-*lacZ* transcriptional fusion at the *amyE* locus.

Partial deletion of the extracellular loop domain results in a constitutively active CssS kinase. Four strains were initially constructed using the system described for Fig. 1A. The wild-type *cssS* gene was reconstituted (strain CB11) to verify that the system functions as predicted (construct A in Fig. 1B). The *cssS* gene in strain CB8 encodes a protein with the N-terminal region and the first transmembrane domain deleted (construct B in Fig. 1B). The *cssS* gene in strain CB9 encodes a protein with an extracellular loop domain of 20 amino acids (amino acids 30 to 39 and 157 to 166 from the amino- and carboxy-terminal regions, respectively, of the extracellular loop) (construct C in Fig. 1B). We call this protein CssS1 and the encoding gene *cssS1*. The *cssS* gene in strain CB10 encodes a protein with the entire sensing domain deleted and is predicted to be cytoplasmically located (construct D in Fig. 1B). The activity of each CssS protein was determined under nonstress conditions and during a secretion stress induced by high-level expression of the heterologous AmyQ α-amylase (the *amyQ* gene is encoded on the multicopy pKTH10 plasmid). Representative results are shown in Table 3. Strains CB11 and CB13 express a reconstituted wild-type CssS protein. There is an ~28-fold increase in P_{htrA}-*lacZ* expression in response to a secretion stress (compare fold induction data for strains CB11 and CB13), an induction level comparable to that observed when wild-type strain 168 was similarly stressed. Thus, we conclude that the system developed to mutate CssS (Fig. 1A) operates as expected. The accumulation of β-galactosidase in the strains expressing CssS with transmembrane 1 (strain CB8; construct B in Fig. 1B) or the entire sensing domain (strain CB10; construct D in Fig. 1B) deleted was only ~2-fold higher than that observed in the strain expressing the reconstituted wild-type CssS protein (strain CB11) in the absence of a secretion stress (Table 3). However, accumulation of β-galactosidase in strain CB9 expressing CssS1 (with a 20-amino-acid extracellular loop domain; construct C in Fig. 1B) was more than 320-fold higher than that observed with the strain CB11 expressing the reconstituted wild-type CssS protein (Table 3). Moreover, this highly elevated level of β-galactosidase in strain CB9 was observed throughout the growth cycle (data not shown) and was not further increased upon exposure to a secretion stress (compare CB9 and CB14 data in Table 3). Importantly, mutating the CssS1 active-site histidine to an alanine residue (strain CB9H H250A; Table 3) completely abolished the high level of β-galactosidase accumulation and secretion stress induction (CB9HQ H250A and pKTH10; Table 3). Western analysis shows the CssS H250A protein to be present in strain CB9H at a level comparable to that of wild-type CssS in strain 168, confirming the loss of increased CssS activity (data not shown). Thus, we infer that the CssS1 kinase protein is constitutively active. These data show that the extracellular loop domain maintains CssS kinase activity at a low level under nonstress conditions and that partial deletion of this domain results in a constitutively active kinase that is unresponsive to secretion stress. Furthermore, it is evident that the secretion stress generated in this study (AmyQ α-amylase overproduction) induced CssS to only ~10% of its maximal (constitutive) activity.

CssS1, CssR, HtrA, and HtrB protein levels are highly elevated in strain CB3 encoding CssS1. The activated CssRS two-component system positively autoregulates its own expression and increases expression of the HtrA and HtrB serine proteases (9). Therefore, HtrA, HtrB, CssR, and CssS1 (truncated by 117 amino acids) protein levels should be highly elevated in strain CB3 expressing CssS1. The levels of these four proteins in strain CB3 (expressing CssS1) were compared with those in strain CB5 (expressing the reconstituted wild-type CssS) by Western analysis using specific polyclonal antibodies. The results are shown in Fig. 2. A band with the predicted size of wild-type CssS protein (top panel, arrow, M_r [54.2]) is present in strain CB5, and its intensity increased between the exponential-growth and stationary phases (OD_{600} of 1, 2, and 4). These mobility and expression profiles of reconstituted CssS in strain CB5 are similar to those of wild-type CssS in strain 168 (data not shown), further supporting the view that the CssS mutation system that was developed (Fig. 1A) functions as predicted. A smaller band of M_r (~25), present in lysates of CB3 harvested at an OD_{600} of 4.0, is likely to be a processed form of CssS. CssS protein was not detected by Western analysis in strain CB2 (CssS construct B in Fig. 1B) or in strain CB4 (CssS construct D in Fig. 1B), indicating that these mutated proteins are probably unstable and degraded (data not shown). However, the CssS1 protein accumulates to a very high level in strain CB3 (Fig. 2, top panel, arrowhead). As expected, the CssS1 protein (strain CB3) is smaller than the full-length CssS protein (strain CB5) due to the 117-amino-acid deletion within the extracellular loop domain (Fig. 2). Notably, the level of CssS1 protein in strain CB3 is elevated throughout the growth cycle, consistent with the constitutive expression of P_{htrA}-*lacZ* observed in strain CB13 (Table 3). Similarly, the cellular levels of CssR (Fig. 2, second panel), HtrA (Fig. 2, third panel), and HtrB (Fig. 2, bottom panel) were all very significantly elevated throughout the growth cycle in strain CB3 (expressing the CssS1 protein) compared to the level observed in strain CB5 (expressing the reconstituted wild-type CssS protein). The faster-migrating bands observed only in strain CB3 may indicate that significant CssRS, HtrA, and HtrB protein degradation occurs due to their elevated cellular levels. We have previously reported that a processed form of HtrA accumulates in the me-

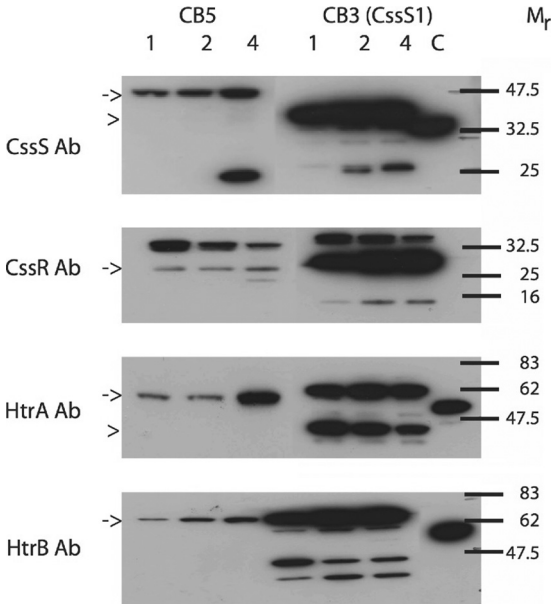

FIG 2 Western analysis of the CssRS operon proteins within strain CB3. Samples were harvested at OD_{600} of ~1, 2, and 4, separated by sodium dodecyl sulfate-polyacrylamide gel electrophoresis (SDS-PAGE), and transferred to membrane and probed with polyclonal antibodies (Ab) directed against CssS, CssR, HtrA, and HtrB. The migration position of each full-length protein is indicated by an arrow, while the migration position of truncated proteins is indicated by an arrowhead. The CssS protein in CB5 is full length and in CB3 is truncated by 117 amino acids, the deletion in the extracellular loop region. The positive-control ′CssS protein is also truncated and contains only the cytoplasmic domain (C). CssR and HtrB are full length in both strains, while HtrA undergoes a processing event that results in a cell-associated full-length and truncated protein. The migration positions of standard proteins are indicated on the right side of the figure with their M_r values.

dium during growth of wild-type strain 168 (2). We found a 200-fold increase in the level of processed HtrA in the culture supernatant of strain CB3 compared to the level found in wild-type strain 168 (data not shown). Clearly, the cellular level of all CssRS regulon proteins is significantly elevated in strains expressing the CssS1 kinase (20-amino-acid extracellular loop domain). We propose that these greatly increased protein levels are due to the formation of an unregulated-feedback expression loop caused by the constitutive CssS1 kinase acting within a positively acting autoregulatory circuit.

Functional analysis of the CssS extracellular loop domain. An alignment of the extracellular loop domains of CssS orthologues from *B. subtilis*, *B. licheniformis*, *B pumilis*, and *B. amyloliquefaciens* is shown in Fig. 3. The amino acids positioned adjacent to the transmembrane helices (26 amino acids at the amino-terminal end and 19 amino acids at the carboxy-terminal end of the extracellular loop) are highly conserved, with some additional conserved amino acid clusters scattered throughout the remainder of the domain. The truncation of the loop domain in the CssS1 protein (the loop is composed of amino acids 30 to 39 followed by amino acids 157 to 166, shown shaded in gray in Fig. 3) removes a significant portion of both conserved regions. Therefore, to refine our analysis of CssS extracellular loop domain function, three approaches were adopted, informed by the conservation profile seen in Fig. 3: (i) deletion of small regions of the loop; (ii) random mutation of the loop by PCR mutagenesis; and (iii) site-directed mutagenesis.

(i) Small deletions within the CssS extracellular loop domain. Three deletions, each of 21 amino acids, were separately made in the N-terminal (amino acids 41 to 61), central (amino acids 86 to 106), and C-terminal (amino acids 131 to 151) regions of the CssS extracellular loop domain (marked in bold in Fig. 3). CssS activity was monitored in the resultant strains (by measuring β-galactosidase accumulation from the P_{hrA}-*lacZ* fusion) in the absence (HA58, HA64, and HA60) and presence (HA70, HA73, and HA71) of secretion stress. CssS activity was measured contemporaneously in control strains CB11, CB12, CB9, and CB14. Representative results are presented in Table 4. Subjecting wild-type cells to a secretion stress increased P_{hrA}-*lacZ* expression ~32-fold as expected (compare data showing β-galactosidase accumulation in strains CB11 and CB12). Moreover, expression of

```
B. licheniformis              STTLQNFFTDEIYTNIENEQHVLTEYGFSDSPERGFGGSSGSRSTN-RHVQHVLLPEKGT
B. pumilis                    SNTLRNFFTNEIYKNIENEQQVLTEYPLNRD------GSPKSTPEN-RSVQHILIPSD-E
B. subtilis  (TM1 10-29)  30 SNTLRDFFTNETYTTIENEQHVLTEYRLPGSIERRYYSEEATAPTTVRSVQHVLLPENEE 89
B. amyloliquefaciens          SNTLRNFFTDETYTTIENEQHVLTEYRLPGSIERGYYSEDATAPTTFRSVQHVLLPQREE
                              *.**::***:* *..*****:***** :  .      ..  : . . * ***:*:*.

B. licheniformis              VYQSP--QILPDSFIEKVQKLGKRQDESSKRYSENVNGEHVFFVLKK-IQTQDQTFLLLS
B. pumilis                    LNQMG--QFFPHAFIEKIQAFVKKQKSATKRYSEEVNGQHIFFVIKK-VSTGNTQYILLS
B. subtilis               90  ASSDKDLSILSSSFIHKVYKLADKQEAKKKRYSADVNGEKVFFVIKKGLSVNGQSAMMLS 149
B. amyloliquefaciens          SASDKDLNYFSSSFIHKVYKLAGRQHSVTKRYSADISGEKVFFVIKKGLTINGQDAMMLS
                                .    . :. :**.*:  :  :*.  .**** ::.*:::***:** :   .   ::**

B. licheniformis              YALDSYRDDLSHTLFKQ
B. pumilis                    YAPDSYRDDLSFTLFKQ
B. subtilis               150 YALDSYRDDLAYTLFKQ (TM2 167 – 186)
B. amyloliquefaciens          YALDSYRDDLAYTLFKQ
                              ** ********:.*****
```

FIG 3 Alignment of the CssS proteins from *B. subtlis* strain 168, *B. amyloliquefaciens* strain FZB42, *B. licheniformis* strain ATCC 14580, and *B. pumilis* SAFR-032. Asterisks signify amino acid identity and colons conservative changes at each position. The amino acids that form the CssS1 (truncated) loop domain are shaded in gray. The 21-amino-acid deletions made in strains HA58, HA64, and HA60 are shown in bold. The positions at which amino acid substitutions L33Q, N47Y, Q49H, D153A, S154A, Y155A, R156A, D157A, and D158A were made are underlined. The sequence replaced by the 3× FLAG tag epitope is shown in red, while the 7-amino-acid deletion (DSYRDDL) is shown in orange. The 20 amino acids preceding (amino acids 10 to 29) and the 20 amino acids succeeding (amino acids 167 to 186) these sequences in *B. subtilis* form transmembrane helices 1 and 2, respectively. Protein identity codes are as follows: *B. subtilis*, NP_391182.2; *B. amyloliquefaciens*, YP_001422575.1; *B. licheniformis*, YP_080579.1; and *B. pumilis*, YP_001488168.1.

TABLE 4 Fold induction of β-galactosidase in *B. subtilis* strains expressing mutated CssS proteins from the natural promoter

Strains (−/+ pKTH10)[a]	CssS mutation	Fold increase in β-galactosidase expression over wild-type CssS induced by amylase[b]		Fold induction of CssS β-galactosidase by amylase[c]
		No pKTH10	+ pKTH10	
CB11/CB12	Wild type	1	32	32
CB9/CB14	ΔECL	343	349	1
HA58/HA70	Δ40–60 AA[d]	327	313	1
HA64/HA73	Δ85–105 AA	98	88	1
HA60/HA71	Δ130–150 AA	27	22	1
HA54/HA68	L33Q	339	325	1
HA62/HA72	N47Y	330	325	1
HA56/HA69	Q49H	271	307	1.1
DN1980/DN1980Q	D153A	<1	1	1
DN1981/DN1981Q	S154A	<1	1	1
DN1982/DN1982Q	Y155A	13	1.5	0.1
DN1983/DN1983Q	R156A	1	1	1
DN1984/DN1984Q	D157A	1	1	1
DN1985/DN1985Q	D158A	2	1	1
DN1986/DN1986Q	Deletion of DSYRDD	16	24	1.5
DN1987/DN1987Q	L33Q R156A	68	77	1
DN1988/DN1988Q	CssSΔ58–79::3×FLAG	76	82	1
DN1991/DN1991Q	CssSΔ61–79::3×FLAG (+ 3AA)	326	354	1

[a] +, strain with plasmid; −, strain without plasmid.
[b] Values represent the extent to which CssS variants are active relative to wild-type CssS.
[c] Values represent the extent to which each CssS variant is induced by amylase (pKTH10).
[d] AA, amino acids.

P_{htrA}-*lacZ* in strains CB9 and CB14 was ~340-fold higher than that observed in nonstressed wild-type cells, consistent with previous results. Each 21-amino-acid deletion within the loop domain affected CssS activity differently. Deletion of the amino-terminal 21-amino-acid segment (strain HA58) increased P_{htrA}-*lacZ* expression ~320-fold, similar to that observed in strain CB9 carrying the constitutively active CssS1 (Table 4). Deletion of the central 21-amino-acid segment (strain HA64) increased P_{htrA}-*lacZ* expression ~98-fold (approximately 1/3 of the level seen in strain CB9), while deletion of the carboxy-terminal 21-amino-acid segment increased P_{htrA}-*lacZ* expression ~27-fold (approximately 1/13 of the level seen in strain CB9). Interestingly, introduction of a secretion stress (strains HA70, HA73, and HA71) did not further increase P_{htrA}-*lacZ* expression relative to that observed in nonstressed strains (strains HA58, HA64, and HA60, respectively; Table 4). The results suggest that these mutated CssS proteins are insensitive to secretion stress. However, an important caveat is that AmyQ overexpression may not generate a secretion stress in cells with elevated HtrA and HtrB protein levels.

(ii) Random mutation of the CssS loop domain. Deletion analysis affects both the amino acid composition and the size of the extracellular loop domain. To distinguish between these two effects, the system described in Fig. 1A was used to randomly introduce amino acid changes specifically into the CssS extracellular loop domain, screening for colonies with increased β-galactosidase expression on X-Gal-containing agar plates. Three strains showed highly elevated β-galactosidase expression, and each had a single amino acid substitution within the CssS loop domain. To ensure that only this single amino acid was changed in each protein, *cssS* alleles encoding these amino acid changes were reconstructed by site-directed mutagenesis (as outlined in Fig. 1A) and inserted into the chromosome to generate strains HA54 (CssS L33Q), HA62 (CssS N47Y), and HA56 (CssS Q49H) (Table 4). β-Galactosidase production increased between 271- and 339-fold in these three strains, a level similar to that observed in strain CB9 expressing CssS1 (117 amino acids deleted from the extracellular loop domain). These results are consistent with and extend the deletion analysis reported in the previous section: all three amino acid substitutions are located within the conserved region of the CssS loop domain juxtaposed to transmembrane helix 1, and two of the three substitutions (N47Y and Q49H) are located within the loop region that is deleted in strain HA58 (amino acids 41 to 61 deleted; Fig. 3). Subjecting each of these strains to secretion stress (by introducing pKTH10 into strains HA54, HA62, and HA56 to generate strains HA68, HA72, and HA69) did not further increase P_{htrA}-*lacZ* expression (Table 4). Thus, each of the three nonconservative amino acid substitutions within this conserved loop region juxtaposed to transmembrane helix 1 was sufficient to generate a constitutively active CssS kinase, showing that this region plays a crucial role in maintaining CssS with very low kinase activity in the absence of secretion stress and in the switch to higher activity upon induction.

(iii) Site-directed mutation of the CssS loop domain. The region of the CssS loop domain flanking transmembrane helix 2 is also highly conserved (Fig. 3). However, mutations were not found in this region in the collection of mutagenized strains. Since only gain-of-function CssS mutants (i.e., increased β-galactosidase production) are detected in our screen, we posited that this region of the CssS loop domain might contribute differently to signal perception and/or transduction. Therefore, an alanine-scanning mutagenesis of the conserved DSYRDD motif was performed and, in addition, a strain expressing CssS with a 7-amino-acid (DSYRDDL) deletion was generated. CssS activity was determined in the resultant strains by measuring expression of the P_{htrA}-*lacZ* fusion in the absence and presence of secretion stress. Representative results are presented in Table 4. Mutation of five of the six amino acids within this conserved CssS region does not result in increased β-galactosidase accumulation. The exceptional case is DN1982 (expressing CssS Y155A), where a small increase (~13-fold) in accumulation was observed that, curiously, was reduced in response to secretion stress. Importantly, CssS kinase activity was not induced by a secretion stress in any of these strains, signifying that they are signal blind (Table 4). Although deletion of 7 amino acids from this region (strain DN1986; deletion of DSYRDDL) resulted in a 16-fold increase in β-galactosidase accumulation under nonstress conditions, there was only marginal induction (1.5-fold) in response to a secretion stress (Table 4). These results show that mutating the conserved region flanking transmembrane helix 2 of the extracellular loop domain abolishes CssS induction by a secretion stress and that it is required for signal perception and/or transduction. Clearly, the conserved regions of the CssS extracellular loop domain flanking the transmembrane helices function differently in signal perception and transduction.

To further investigate the different functions of the conserved

loop regions juxtaposed to the transmembrane helices, we constructed a strain expressing CssS that combined the L33Q gain-of-function mutation (confers constitutive noninducible kinase activity) and the R156A loss-of-function mutation (confers low noninducible kinase activity). We found that β-galactosidase accumulation increased 68-fold and 77-fold in the absence (DN1987) and presence (DN1987Q) of secretion stress, respectively, compared to the noninduced CB11 (reconstituted wild-type CssS) strain (Table 4). However, Western analysis showed that this CssS variant was unstable: combining the R156A and L33Q mutations reduced the very high level of protein observed in cells expressing CssS L33Q to approximately the level of CssS observed in noninduced wild-type cells. We posit that the increased P_{htrA}-*lacZ* expression in strains DN1987 and DN1987Q may have been due to a low steady-state level of constitutively active kinase, the residue of the competing processes of high-level expression and protein degradation.

(iv) Replacement of a nonconserved region of the CssS loop domain with the heterologous 3× FLAG epitope. To assess the importance of amino acid identity within the relatively nonconserved region of the CssS loop domain, we replaced a 22-amino-acid segment (amino acids 59 to 80; shown in red in Fig. 3) with a heterologous 3× FLAG epitope of identical length and monitored CssS activity in the absence and presence of secretion stress. As shown in Table 4, this substitution resulted in a partially constitutively active CssS kinase (76- to 82-fold elevated activity) that is unresponsive to secretion stress. Interestingly, replacing the same amino acids with 3× FLAG and increasing the size of the loop domain by 3 amino acids (amino acids GSI; indicated in red bold in Fig. 3) generated a constitutively active CssS kinase (326- to 354-fold elevated activity).

In summary, these studies show that individual regions of the CssS extracellular loop domain function differently in signal perception and transduction. The conserved region adjacent to transmembrane helix 1 is likely to be involved in maintaining the CssS kinase in a low activity state under nonstress conditions and in the switch to increased activity in response to secretion stress. The conserved region adjacent to transmembrane helix 2 is required for signal sensing and/or signal transduction, since all mutations in this region render CssS signal blind. The size of the extracellular loop was also important, since all perturbations led to an increase (27- to 343-fold; Table 4) in CssS activity.

Mutation of the CssS loop domain in strains lacking the positive autoregulatory loop of *cssRS* expression. The positive autoregulation of *cssRS* expression amplified the effects of gain-of-function mutations (e.g., L33Q), resulting in very high cellular CssS levels, while loss-of-function mutations (e.g., D153A) resulted in low cellular CssS levels. Such a disparity in protein levels complicates a comparison of the activities of different CssS variants. To address this issue, we placed *cssRS* expression under the control of the IPTG-inducible P_{spac} promoter (thereby removing the autoregulatory loop), allowing us to compare the effects of selected mutations in the loop domain in strains with comparable cellular CssS protein levels. All such strains were grown with addition of 100 μM IPTG, a level of inducer that significantly increased the cellular level of CssS protein (Fig. 4; compare strain 168D with 168E and strain 168DQ with 168EQ). CssS protein levels were very similar in all strains (except DN1987) expressing *cssRS* from the P_{spac} promoter, regardless of the presence or absence of pKTH10 (compare strains in Fig. 4A with those in Fig. 4B), showing that the autoregulatory loop had been removed and that expression was no longer inducible by secretion stress. Importantly, the level of CssS protein in cells expressing gain-of-function (Fig. 4 [HA54C, HA54CQ, HA62C, and HA62CQ]) and loss-of-function (Fig. 4 [DN1980C, DN1980CQ, and DN1984CQ]) variants was very similar to that in cells expressing wild-type protein (168E and 168EQ; Fig. 4), showing that neither type of mutation destabilized CssS protein and allowing direct comparison of their activities (Table 5). Increasing the CssS protein level in wild-type strain 168E ~20-fold (Fig. 4) increased the noninduced level of P_{htrA}-*lacZ* expression only ~3-fold (compare strains 168D and 168E; Table 5). However, applying a secretion stress (strain 168 EQ) in this background increased P_{htrA}-*lacZ* expression only 19-fold, very similar to the 16-fold-increased expression observed in the wild-type background (strain 168DQ), showing that CssRS levels are not limiting in wild-type cells (Table 5). Expression of P_{htrA}-*lacZ* in strains with gain-of-function CssS variants (HA54C, HA54CQ, HA62C, and HA62C) was elevated more than 100-fold, confirming increased CssS kinase activity and showing that the positive autoregulatory loop makes an approximately 3-fold contribution (e.g., compare HA54C and HA62C in Table 5 with HA54 and HA62, respectively, in Table 4) to expression. However, expression of P_{htrA}-*lacZ* in strains with loss-of-function CssS variants (DN1980C, DN1980CQ, and DN1984C) was similar to that in a strain with wild-type CssS (168E) and was not induced by secretion stress, signifying that mutations in this region of the loop domain made the protein signal blind and/or incapable of transducing the signal (Table 5). We were unable to establish plasmid pKTH10 in strain DN1984C, indicating that the cell is unable to mount a secretion stress response. Generally, we found that strains expressing gain-of-function CssS variants (e.g., HA54, HA62) were more readily transformed with pKTH10 than wild-type cells whereas strains expressing loss-of-function CssS variants that are

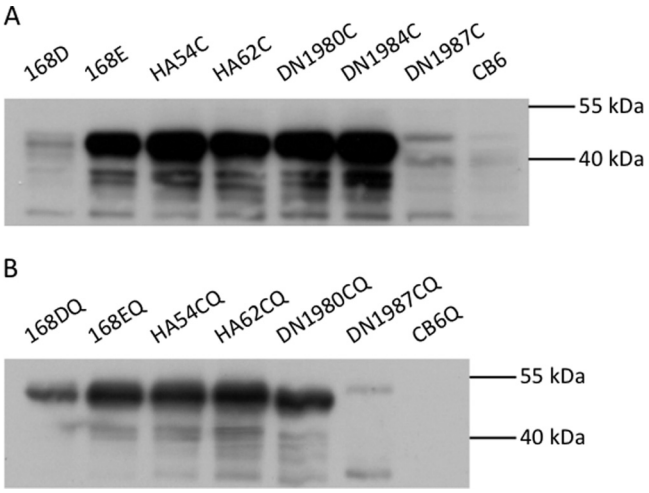

FIG 4 Western blot analysis of CssS protein levels in strains expressing CssS under the control of the IPTG-inducible P_{spac} promoter. Cultures were grown to an OD_{600} of ~2.0 and harvested, and lysates were prepared for SDS-PAGE as described in the text. Lysate samples containing 10 μg for protein were loaded onto each lane, and CssS protein was detected as described in the text. (A) Strains in the absence of a secretion stress (no pKTH10 plasmid). (B) Strains with secretion stress (containing pKTH10 plasmid). Strains CB6 and CB6Q are the negative controls, having the *cssS* gene deleted. The filter was exposed to film for 30 s. Protein sizes are shown at the side of the image.

TABLE 5 Fold induction of β-galactosidase in *B. subtilis* strains expressing mutated CssS proteins under the control of the Pspac promoter

Strains (−/+ pKTH10)[a]	CssS mutation	Fold increase in expression over wild-type CssS induced by amylase[b]		Fold induction of CssS by amylase[c]
		No pKTH10	+ pKTH10	
168D/168DQ	Wild type	1	16	16
168E/168EQ	Wild-type CssS under Pspac control	3	19	6
HA54C/HA54CQ	CssS L33Q under Pspac control	117	100	0.85
HA62C/HA62CQ	CssS B47Y under Pspac control	129	106	0.82
DN1980C/DN1980CQ	CssS D153A under Pspac control	3.3	3.8	1.1
DN1984C/SNO	CssS D157A under Pspac control	3.1	ND	
DN1987C/DN1987CQ	CssS L33Q R156A under Pspac control	63	49	0.8

[a] +, strain with plasmid; −, strain without plasmid; SNO, strain not obtained.
[b] Values represent the extent to which CssS variants are active relative to wild-type CssS. ND, not determined.
[c] Values represent the extent to which each CssS variant is induced by amylase (pKTH10).

unresponsive to secretion stress (e.g., CB6, DN1980C, DN1984C) were very poorly transformable, if at all, with pKTH10. These analyses also confirm that combining the L33Q gain-of-function mutation with the loss-of-function R156A, neither of which affects protein stability individually, destabilized CssS, with only a low level of full-length protein detectable by Western analysis (DN1987C and DN1987CQ; Fig. 4). In summary, these data confirm that the conserved regions of the CssS loop domain adjacent to the transmembrane helices function differently in signal perception, activation, and transduction.

Localization of the CssS, HtrA, and HtrB proteins in *B. subtilis*. We established the cellular localization of CssS, HtrA, and HtrB by immunofluorescence in exponentially growing *B. subtilis* cells (Fig. 5). CssS is primarily located at the septa of dividing cells and at the poles of many cells (Fig. 5A to C). Two separate but juxtaposed CssS bands positioned at the septa and poles of cells that are dividing or have just divided are shown in Fig. 5A. Some cells also showed a punctate distribution of CssS along the cell cylinder but with lower intensity (Fig. 5C). A minority of cells showed no staining (see, e.g., Fig. 5B): it is unclear whether this result represents cells not expressing CssRS or whether there was insufficient antibody penetration for visualization. We conclude from these and many additional images that CssS is localized at the septa of dividing cells and in a punctate manner along the cell cylinder.

HtrA was located at only one or a few foci in exponentially growing wild-type 168 cells but was not detected in all cells (Fig. 5D). This is consistent with our demonstration that HtrA is expressed at low levels in nonstressed cells and that it is processed and shed into the medium during growth (2, 34, 35). The number of HtrA foci increased very significantly in cells expressing very high HtrA levels (strain HA54, expressing the constitutively active CssS L33Q), and the foci were distributed along the length of the cell cylinder in an apparently random manner (Fig. 5E). In addition, a lower level of continuous fluorescence covers the entire surface of cells of strain HA54, suggesting that the very high level of HtrA saturated all potential focal binding sites and that surplus protein became evenly distributed over the cell surface. HtrB was also located in foci distributed throughout the length of wild-type 168 cells in an apparently random manner (Fig. 5F). Importantly,

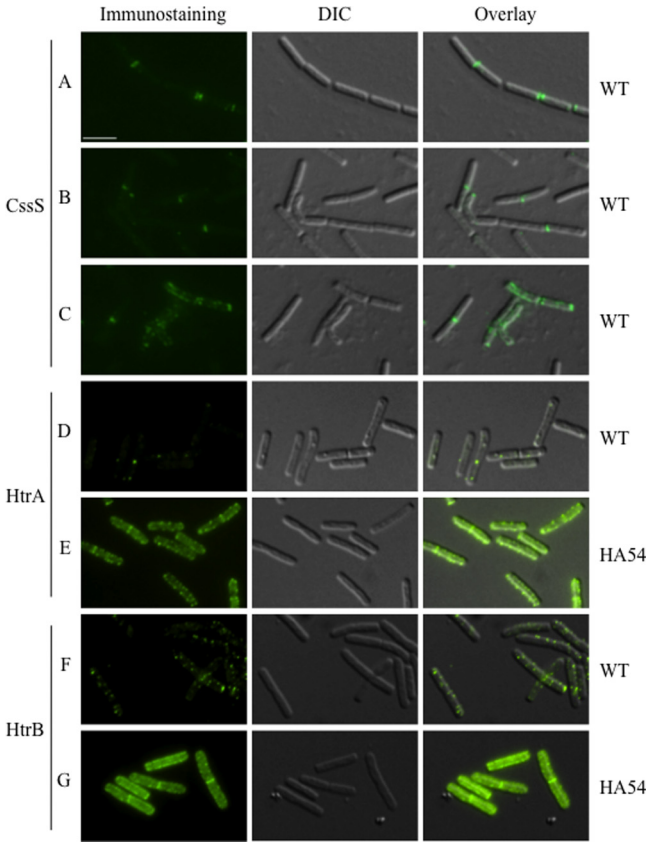

FIG 5 Localization of the CssS, HtrA, and HtrB proteins in *B. subtilis*. The CssS, HtrA, and HtrB proteins were visualized by differential interference contrast microscopy (DIC) and by immunostaining (immunofluorescence) microscopy in nonstressed wild-type strain 168 and in strain HA54 (CssS L33Q) cells that express a constitutive CssS kinase. CssS (A, B, and C) was visualized by staining with an anti-myc-tag antibody, while HtrA (D and E) and HtrB (F and G) were stained with specific affinity-purified polyclonal antisera. Visualization of primary antibodies was performed by staining with a fluorescein isothiocyanate (FITC)-labeled secondary antibody. Bar, 4 μm for all images.

HtrB foci were observed in the vast majority of cells, while the number of HtrB foci per cell was also significantly higher than the number of HtrA foci. The number of HtrB foci was elevated in strain HA54 (expressing constitutively active CssS L33Q) compared with wild-type strain 168 (Fig. 5G). Like HtrA, the entire surface of HA54 cells was covered with a continuous lower level of fluorescence, again suggesting that all potential focal binding sites were saturated and the HtrB surplus protein became evenly distributed over the entire cell surface (Fig. 5G). These data show that HtrA and HtrB were confined to discrete foci on the surface of nonstressed cells. HtrB was present at most of the potential binding site foci in nonstressed cells, whereas HtrA was largely absent from the cell surface under this condition, probably because it was processed and shed into the medium (2). However, increasing HtrA expression showed many additional foci to which it could bind. Moreover, when highly expressed, both proteins were also evenly distributed at a lower level throughout the cell length. In view of the fact that CssS localizes primarily to cell septa and poles, it is interesting that neither HtrA nor HtrB showed septal or polar localization.

DISCUSSION

The CssS kinase is a member of the EnvZ/OmpR family of kinases that has two transmembrane helices flanking a 137-amino-acid extracellular loop proposed to encode a PAS domain (6, 31). While CssS responds to heat and secretion stress stimuli, the identity of the signal, how it is perceived by CssS, and how perception activates kinase activity are largely unknown. Here we have identified several features of the extracytoplasmic loop domain that are important for signaling. The extracytoplasmic loop domain functions to maintain the activity of CssS kinase at a very low level in the absence of signal. Deletion of 117 amino acids from the extracytoplasmic loop domain (CssS1) increased kinase activity more than 300-fold even in the absence of secretion stress. CssS1 appears to be unresponsive to stress, although it must be remembered for all strains showing increased CssS kinase activity that AmyQ overexpression may not generate a secretion stress in cells having highly elevated levels of HtrA and HtrB proteases. Thus, the nonstressed (P_{htrA}-*lacZ* expression similar to that in *cssS* null strains) and CssS1 (P_{htrA}-*lacZ* expression increased 300-fold) protein states appear to be the extremities of CssS kinase activity, representing the "off" and "on" conditions, respectively, in the cell. It is interesting that the heat and secretion stresses (P_{htrA}-*lacZ* expression increased 6- and 25-fold, respectively [reference 35 and this study]) induced CssS kinase activity to a level at the lower end of its capability. The CpxRA two-component system also responds to cell envelope and secretion stresses in *E. coli* (10, 43). In a manner similar to that seen with CssS, an in-frame deletion of 32 amino acids in the central region of the CpxA periplasmic sensing domain (CpxA24) results in a gain of function, renders it insensitive to secretion stress, and results in a significantly elevated level of CpxRA protein in the cell due to positive autoregulation of the *cpxRA* operon (38, 40). Thus, the negative role of the periplasmic sensing domain and amplification of the signal through positive autoregulation are themes common to the CssRS (of *B. subtilis*) and CpxRA (of *E. coli*) two-component systems in the detection and response to secretion stresses. However, this is not universal among two-component systems, since deletion of the extracellular loop (encoding a PAS domain) of PhoR in *B. subtilis* does not result in constitutive activity or render it insensitive to detecting phosphate limitation (E. Botella and K. M. Devine, unpublished results).

The two regions of the CssS extracellular loop domain that are juxtaposed to the transmembrane helices are highly conserved among CssS orthologues of closely related bacilli (Fig. 3) and have distinct functions. The 26-amino-acid region that is adjacent to transmembrane helix 1 functions in the activity switch that occurs upon cognate stimulus detection. In the absence of signal, this region functions to maintain the CssS kinase in a low activity state. However, single nonconservative amino acid substitutions (L33Q, N47Y, Q49H) in this region generate CssS variants that are constitutively active. Interestingly, Raivio and Silhavy (38) also reported a gain-of-function mutation (*cpxA104*) localized to this region of the CpxA loop domain. The amino acid composition of this CssS region is very hydrophilic, with 9 hydroxyl groups (Ser, Thr, and Tyr), 5 carboxyl groups (Asp and Glu), 2 positive charges (Arg and His), and 4 amide groups (Gln and Asn). Among the remaining 6 hydrophobic amino acids, there is an unusual pair of adjacent Phe residues. The L33Q mutation is especially interesting, since the hydrophobic Leu is directly adjacent to the transmembrane helix (amino acids 10 to 29), while the mutation places the more hydrophilic glutamine at this position. It is tempting to speculate that this conserved hydrophilic domain interacts with the outer leaftlet or face of the cytoplasmic membrane to maintain CssS in a state of low kinase or high phosphatase activity. Signal perception (or mutation, as in this study) may disrupt these interactions, thereby facilitating activation of CssS by increasing kinase or decreasing phosphatase activity.

The role of the conserved 19-amino-acid region adjacent to transmembrane helix 2 in signal perception is distinct from that of the conserved region adjacent to transmembrane helix 1. CssS variants mutated in this region are signal blind and have activities similar to those of the noninduced wild-type CssS protein. Thus, this region is required for either signal perception and/or transduction. CssS differs from CpxA in that all point mutations in this CssS region are inactive and signal blind whereas the CpxA103 (R164P) variant mutated in this region has increased activity, although it is also signal blind. The strain expressing the CssS L33Q R156A double-mutant variant (DN1987) is especially interesting. Expression of each CssS single-mutant variant shows that both proteins are stable. However, the CssS variant with both mutations (DN1987C and DN1987CQ) is highly unstable, with only a low level of full-length CssS visible and extensive protein degradation being observed. The size of the loop domain and features located between these two conserved membrane-associated domains are also important for signal perception. All size perturbations of the loop domain increase CssS activity. Moreover, changing the amino acid composition of part of the loop domain (by replacement of 22 amino acids with a 22-amino-acid 3× FLAG tag) increased CssS activity 76-fold. When this replacement was combined with a 3-amino-acid increase in the size of the loop domain, CssS activity increased 326-fold, similar to that observed when most of the loop domain was deleted.

It is not possible to ascertain the effect of these perturbations on the various enzymatic activities of the CssS kinase because of difficulties in purifying integral membrane proteins and because such activities probably depend on proper membrane localization. Kinases such as CssS and CpxA have autophosphorylation, phosphotransfer, and phosphatase enzymatic activities. Thus, while the mutated CssS proteins in this study had altered activities,

it is not possible to determine the mechanism by which they arise to give the phenotypes that we observe. Raivio and Silhavy (38) have shown through *in vitro* analysis that the gain-of-function CpxA101 (T253P) variant retains kinase activity but that it lacks phosphatase activity. By analogy with their work, our gain-of-function CssS variants might have altered the kinase/phosphatase ratio by either increasing kinase or decreasing phosphatase activity. However, such mechanistic analysis awaits technical advances allowing enzymatic changes to be determined with full-length kinases correctly positioned in lipid bilayers.

The importance to signaling of the loop regions positioned adjacent to transmembrane helices has been observed in systems additional to the Cpx system already mentioned. In the PhoPQ two-component system, which responds to magnesium ions and antimicrobial peptides, there is an acidic region at one side of the PhoQ periplasmic loop domain that is tethered to the face of the plasma membrane by cations rendering the kinase inactive. The inducing antimicrobial peptides are proposed to disrupt the membrane binding by displacing the cations, thereby levering this protein region away from the membrane and activating the PhoQ kinase activity (3, 7, 27, 31). In the NarXL two-component system of *E. coli* that responds to nitrate or nitrite, the NarX kinase has a extracellular loop domain of ~100 amino acids with two conserved 19-amino-acid boxes (called the P- and P′-box) located adjacent to the cytoplasmic membrane. Mutation of the P-box conferred impaired NarXL induction and had a constitutive phenotype, whereas mutation of the P′-box displayed no phenotype (45). A recent study showed that, in the VanRS two-component system of *Streptomyces coelicolor*, vancomycin directly binds to the N-terminal region (amino acids 1 to 41) of the VanS histidine kinase of *S. coelicolor* that comprises the first transmembrane helix and 4 amino acids (DQGW) of the extracytoplasmic loop domain (26). It is interesting that the L33Q mutation that generates a constitutive active CssS is positioned within the same region of the extracellular loop as these 4 amino acids of VanS. Thus, despite the diversity in the stimulus (antimicrobial peptides, nitrate/nitrite, vancomycin, and secretion stress), the region of the extracytoplasmic loop domain juxtaposed to transmembrane helix 1 emerges as being important for signal perception and activation of the kinase.

Two approaches were employed to identify proteins that might interact with CssS to maintain it in a state of low kinase activity: immunoprecipitation of CssS cross-linked with other proteins and transposon mutagenesis screening for a gain-of-function (high-level P_{htrA}-*lacZ* expression) phenotype (data not shown). Both approaches were unsuccessful. However, the transposition study showed that sufficient transposants were screened to identify a protein that interacts with the CssS loop domain to maintain it in a low-activity state: e.g., we identified a number of transposants with insertions into *htrA* and *htrB* as expected (35, 36). These results suggest that the loop domain of the CssS kinase may interact with more than one protein (perhaps in a protein complex) or that the protein(s) with which it interacts is essential.

The CssS kinase is located primarily at cell septa and the poles of divided cells. The observation of a lower punctate distribution along the cylinder suggests that it may also be distributed throughout the cell under some conditions. The septal location is especially interesting in view of the recent finding that peptidoglycan recognition proteins (PGLYRPs) bind to cell separation sites in both *B. subtilis* and *E. coli* and activate the CssRS and CpxRA two-component systems, respectively (24). Binding of PGLYRPs kills cells by depolarizing membranes, leading to decreased peptidoglycan DNA and RNA synthesis and production of hydroxyl radicals (24). In view of the viability of *B. subtilis* cells with a constitutively active CssRS system, it is likely that CssRS activation is a consequence of PGLYRP-mediated cell envelope perturbation rather than the direct cause of cell death. The HtrA and HtrB proteins are located at discrete foci randomly distributed along the *B. subtilis* cell surface. Unstressed cells have many more HtrB foci than HtrA foci, which is consistent with our previous observations that HtrB remains cell associated whereas HtrA is cleaved and shed into medium (2). The amount of cell-associated HtrA and HtrB increases dramatically when the level of both proteins is elevated (in strain HA54, containing CssS L33Q): in particular, the number of HtrA foci increases significantly when the level of HtrA protein is increased, showing that potential HtrA binding foci exist in such cells but that it does not remain bound to them. In addition, there is an evenly distributed lower level of HtrA and HtrB bound to HA54 cells, suggesting that surplus protein can remain attached to sites other than the foci. It is indeed interesting that CssS appears to be distributed quite differently from the HtrA and HtrB chaperone proteases. This suggests that the sites at which the stress signal is generated and detected by CssS are quite different from the sites at which the HtrA and HtrB proteases are required to deal with it. Restriction of HtrA and HtrB to specific locations of the surface is similar to the situation in *Streptococcus pyogenes*, where HtrA is associated with ExPortal, a single region of the cell surface containing the secretion apparatus (42). It will be interesting to establish whether HtrA and HtrB are similarly associated with the secretion apparatus in *B. subtilis*.

ACKNOWLEDGMENTS

This work was supported by grants 03/IN3/B409 and 08/IN.1/B1859 from Science Foundation Ireland, by BACELL Health grant LSHG-CT-2004-503468, and by BaSysBio grant LSHG-CT-2006-037469.

REFERENCES

1. **Anagnostopoulos C, Spizizen J.** 1961. Requirements for transformation in *Bacillus subtilis.* J. Bacteriol. **81**:741–746.
2. **Antelmann H, et al.** 2003. The extracellular proteome of *Bacillus subtilis* under secretion stress conditions. Mol. Microbiol. **49**:143–156.
3. **Bader MW, et al.** 2005. Recognition of antimicrobial peptides by a bacterial sensor kinase. Cell **122**:461–472.
4. **Bantscheff M, et al.** 2000. Structure-function relationships in the Bvg and Evg two-component phosphorelay systems. Int. J. Med. Microbiol. **290**: 317–323.
5. **Bisicchia P, et al.** 2007. The essential YycFG two-component system controls cell wall metabolism in Bacillus subtilis. Mol. Microbiol. **65**:180–200.
6. **Chang C, et al.** 2010. Extracytoplasmic PAS-like domains are common in signal transduction proteins. J. Bacteriol. **192**:1156–1159.
7. **Cho US, et al.** 2006. Metal bridges between the PhoQ sensor domain and the membrane regulate transmembrane signaling. J. Mol. Biol. **356**:1193–1206.
8. **Cotter PA, Jones AM.** 2003. Phosphorelay control of virulence gene expression in *Bordetella.* Trends Microbiol. **11**:367–373.
9. **Darmon E, et al.** 2002. A novel class of heat and secretion stress-responsive genes is controlled by the autoregulated CssRS two-component system of *Bacillus subtilis.* J. Bacteriol. **184**:5661–5671.
10. **Dorel C, Lejeune P, Rodrigue A.** 2006. The Cpx system *of Escherichia coli*, a strategic signaling pathway for confronting adverse conditions and for settling biofilm communities? Res. Microbiol. **157**:306–314.
11. **Dubrac S, Bisicchia P, Devine KM, Msadek T.** 2008. A matter of life and death: cell wall homeostasis and the WalKR (YycGF) essential signal transduction pathway. Mol. Microbiol. **70**:1307–1322.
12. **Fukushima T, Szurmant H, Kim EJ, Perego M, Hoch JA.** 2008. A sensor

histidine kinase co-ordinates cell wall architecture with cell division in *Bacillus subtilis.* Mol. Microbiol. **69**:621–632.
13. **Fukushima T, et al.** 2011. A role for the essential YycG sensor histidine kinase in sensing cell division. Mol. Microbiol. **79**:503–522.
14. **Gao R, Stock AM.** 2009. Biological insights from structures of two-component proteins. Annu. Rev. Microbiol. **63**:133–154.
15. **Gerharz T, Reinelt S, Kaspar S, Scapozza L, Bott M.** 2003. Identification of basic amino acid residues important for citrate binding by the periplasmic receptor domain of the sensor kinase CitA. Biochemistry **42**:5917–5924.
16. **Gibson TJ.** 1984. Studies on the Epstein-Barr virus genome. University of Cambridge, Cambridge, United Kingdom.
17. **Glaser P, et al.** 1993. *Bacillus subtilis* genome project: cloning and sequencing of the 97 kb region from 325 degrees to 333 degrees. Mol. Microbiol. **10**:371–384.
18. **Guérout-Fleury AM, Shazand K, Frandsen N, Stragier P.** 1995. Antibiotic-resistance cassettes for *Bacillus subtilis.* Gene **167**:335–336.
19. **Hoch JA, Silhavy TJ (ed).** 1995. Two-component signal transduction. ASM Press, Washington, DC.
20. **Howell A, et al.** 2003. Genes controlled by the essential YycG/YycF two-component system of *Bacillus subtilis* revealed through a novel hybrid regulator approach. Mol. Microbiol. **49**:1639–1655.
21. **Howell A, Dubrac S, Noone D, Varughese KI, Devine KM.** 2006. Interactions between the YycFG and PhoPR two-component systems in *Bacillus subtilis*: the PhoR kinase phosphorylates the non-cognate YycF response regulator upon phosphate limitation. Mol. Microbiol. **59**:1199–1215.
22. **Hyyryläinen HL, et al.** 2001. A novel two-component regulatory system in *Bacillus subtilis* for the survival of severe secretion stress. Mol. Microbiol. **41**:1159–1172.
23. **Hyyryläinen HL, Sarvas M, Kontinen VP.** 2005. Transcriptome analysis of the secretion stress response of *Bacillus subtilis.* Appl. Microbiol. Biotechnol. **67**:389–396.
24. **Kashyap DR, et al.** 2011. Peptidoglycan recognition proteins kill bacteria by activating protein-sensing two component systems. Nat. Med. **17**:676–683.
25. **Kaspar S, et al.** 1999. The periplasmic domain of the histidine autokinase CitA functions as a highly specific citrate receptor. Mol. Microbiol. **33**:858–872.
26. **Koteva K, et al.** 2010. A vancomycin photoprobe identifies the histidine kinase VanSsc as a vancomycin receptor. Nat. Chem. Biol. **6**:327–329.
27. **Krell T, et al.** 2010. Bacterial sensor kinases: diversity in the recognition of environmental signals. Annu. Rev. Microbiol. **64**:539–559.
28. **Kunst F, et al.** 1997. The complete genome sequence of the gram-positive bacterium *Bacillus subtilis.* Nature **390**:249–256.
29. **Leonardo MR, Forst S.** 1996. Re-examination of the role of the periplasmic domain of EnvZ in sensing of osmolarity signals in *Escherichia coli.* Mol. Microbiol. **22**:405–413.
30. **Lulko AT, et al.** 2007. Production and secretion stress caused by overexpression of heterologous alpha-amylase leads to inhibition of sporulation and a prolonged motile phase in *Bacillus subtilis.* Appl. Environ. Microbiol. **73**:5354–5362.
31. **Mascher T, Helmann JD, Unden G.** 2006. Stimulus perception in bacterial signal-transducing histidine kinases. Microbiol. Mol. Biol. Rev. **70**:910–938.
32. **Mascher T, Margulis NG, Wang T, Ye RW, Helmann JD.** 2003. Cell wall stress responses in *Bacillus subtilis*: the regulatory network of the bacitracin stimulon. Mol. Microbiol. **50**:1591–1604.
33. **Miller JH.** 1972. Experiments in molecular genetics, p 431–432. Cold Spring Harbor Laboratory Press, Cold Spring Harbor, NY.
34. **Möglich A, Ayers RA, Moffat K.** 2009. Structure and signaling mechanism of Per-ARNT-Sim domains. Structure **17**:1282–1294.
35. **Noone D, Howell A, Devine KM.** 2000. Expression of *ykdA*, encoding a *Bacillus subtilis* homologue of HtrA, is heat shock inducible and negatively autoregulated. J. Bacteriol. **182**:1592–1599.
36. **Noone D, Howell A, Collery R, Devine KM.** 2001. YkdA and YvtA, HtrA-like serine proteases in *Bacillus subtilis*, engage in negative autoregulation and reciprocal cross-regulation of *ykdA* and *yvtA* gene expression. J. Bacteriol. **183**:654–663.
37. **Palva I.** 1982. Molecular cloning of the alpha-amylase gene from *Bacillus amyloliquefaciens* and its expression in *Bacillus subtilis.* Gene **19**:81–87.
38. **Raivio TL, Silhavy TJ.** 1997. Transduction of envelope stress in *Escherichia coli* by the Cpx two-component system. J. Bacteriol. **179**:7724–7733.
39. **Raivio TL, Silhavy TJ.** 1999. The σE and Cpx regulatory pathways: overlapping but distinct stress responses. Curr. Opin. Microbiol. **2**:159–165.
40. **Raivio TL, Popkin DL, Silhavy TJ.** 1999. The Cpx envelope stress response is controlled by amplification and feedback inhibition. J. Bacteriol. **181**:5263–5272.
41. **Reinelt S, Hofmann E, Gerharz T, Bott M, Madden DR.** 2003. The structure of the periplasmic ligand-binding domain of the sensor kinase CitA reveals the first extracellular PAS domain. J. Biol. Chem. **278**:39189–39196.
42. **Rosch JW, Caparon MG.** 2005. The ExPortal: an organelle dedicated to the biogenesis of secreted proteins in *Streptococcus pyogenes.* Mol. Microbiol. **58**:959–968.
43. **Ruiz N, Silhavy TJ.** 2005. Sensing external stress: watchdogs of the *Escherichia coli* cell envelope. Curr. Opin. Microbiol. **8**:122–126.
44. **Sambrook J, Fritsch EF, Maniatis T.** 1989. Molecular cloning: a laboratory manual, 2nd ed. Cold Spring Harbor Laboratory Press, Cold Spring Harbor, NY.
45. **Stewart V.** 2003. Nitrate- and nitrite-responsive sensors NarX and NarQ of proteobacteria. Biochem. Soc. Trans. **31**:1–10.
46. **Szurmant H, Mohan MA, Imus PM, Hoch JA.** 2007. YycH and YycI interact to regulate the essential YycFG two-component system in *Bacillus subtilis.* J. Bacteriol. **189**:3280–3289.
47. **Szurmant H, White RA, Hoch JA.** 2007b. Sensor complexes regulating two-component signal transduction. Curr. Opin. Struct. Biol. **17**:706–715.
48. **Szurmant H, Fukushima T, Hoch JA.** 2007. The essential YycFG two-component system of *Bacillus subtilis.* Methods Enzymol. **422**:396–417.
49. **Szurmant H, Bu L, Brooks CL III, Hoch JA.** 2008. An essential sensor histidine kinase controlled by transmembrane helix interactions with its auxiliary proteins. Proc. Natl. Acad. Sci. U. S. A. **105**:5891–5896.
50. **Wecke T, Bauer T, Harth H, Mäder U, Mascher T.** 2011. The rhamnolipid stress response of Bacillus subtilis. FEMS Microbiol. Lett. **323**:113–123.
51. **Westers H, et al.** 2006. The CssRS two-component regulatory system controls a general secretion stress response in *Bacillus subtilis.* FEBS J. **273**:3816–3827.